Aptamer biosensor for label-free impedance spectroscopy detection of proteins based on recognition-induced switching of the surface charge†

Marcela C. Rodriguez, Abdel-Nasser Kawde and Joseph Wang*

Received (in Cambridge, UK) 11th May 2005, Accepted 14th June 2005
First published as an Advance Article on the web 12th July 2005
DOI: 10.1039/b506571b

The recognition of proteins by aptamer-modified electrode transducers reverses the surface charge and leads to a novel label-free impedance spectroscopy bioelectronic detection protocol based on a decrease in the electron transfer resistance.

Aptamers are artificial nucleic acid ligands, selected through combinatorial libraries to bind specifically target molecules.[1–3] The remarkable target diversity, tight-binding capability, ease-of synthesis and high stability of aptamers hold great promise for biosensing of toxins or disease-related proteins and for developing protein arrays. Most aptamer-based biosensors reported to date rely on standard sandwich bioaffinity assays in connection to common enzyme,[4] fluorophore,[5,6] or nanoparticle[7,8] tracers. Yet, the different nature of these nucleic-acid recognition elements and their protein targets, and the unique properties of aptamers, indicate great promise for designing innovative sensing protocols.[9,10]

Here we describe a novel label-free bioelectronic strategy for transducing aptamer–protein recognition events based on recognition-induced reversal of the surface charge for electrostatically controlling access of redox marker ions used in Faradaic Impedance Spectroscopy (FIS) signal transduction. FIS is an effective method for probing protein binding events such as antibody–antigen interactions.[11–13] The formation of such bioaffinity complexes commonly leads to an insulating layer that retards the interfacial electron transfer kinetics between the redox probe and the electrode and increases the electron-transfer resistance. Contrary to impedance-based immunoassays, we demonstrate below that (with a proper pH control) the aptamer–protein interaction leads to a decrease (rather than the common increase) in the electron transfer resistance.

As illustrated in Fig. 1, the negatively-charged aptamer probe acts as an electrostatic barrier that repels the $[Fe(CN)_6]^{3-/4-}$ marker and hinders its interfacial electron transfer reaction (A); the selective binding of the protein to the aptamer-functionalized electrode (using pH below the pI) results in switching of the surface charge and provides an excess positive charge, that facilitates access of the marker and its redox reaction (B). Such unique recognition-induced reversal of the surface charge (and switching from repulsion to attraction of the redox marker) lead to a highly sensitive label-free electronic signaling of aptamer–protein binding

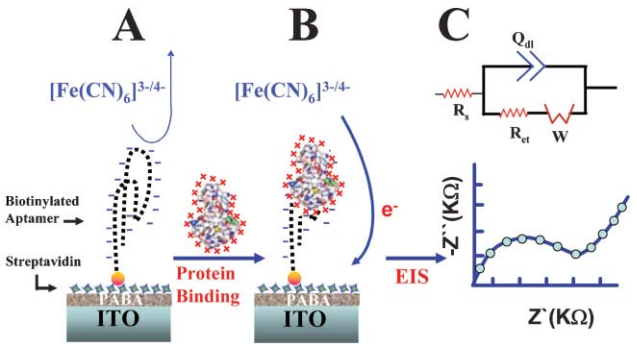

Fig. 1 Schematic illustration of the label-free FIS biosensing of proteins at the aptamer-functionalized ITO electrode. Without the target protein the negatively-charged $[Fe(CN)_6]^{3-/4-}$ marker is repelled from the surface and its redox reaction is hindered (A). When the protein binds to the aptamer probe, the $[Fe(CN)_6]^{3-/4-}$ marker is attracted to the surface and the resistance to electron transfer is decreased (B). Equivalent circuit $R_s(Q_{dl}[R_{et}W])$ used to fit the frequency scans along with a FIS response (C). R_s is the solution resistence, R_{et} is the electron-transfer resistance, Q_{dl} is a constant phase element modeling the double layer capacitance and W is the Warburg impedance element. (Relative sizes of ITO electrode, PABA polymer layer, streptavidin, anti-lysozyme biotinylated aptamer and lysozyme are not in scale.) See Supplementary Information† for experimental details.

events and makes aptamer recognition elements ideally suited for label-free FIS biosensing. Fig. 1 outlines the steps involved in the new protocol. These include the immobilization of the biotin-conjugated aptamer onto the streptavidin/polymer-coated indium–tin oxide (ITO) electrode, and comparing the FIS response before (A) and after (B) incubation in the presence of the protein sample drop solution, along with different washing steps. While ITO electrodes were employed due to their stability and compatibility with microfabrication, other materials can be used. See Electronic Supplementary Information† for experimental details.

Measurements of lysozyme (pI = 11)[14] were used to demonstrate the new label-free impedance detection in connection to an anti-lysozyme coated ITO electrode and a phosphate buffer (pH 7.0) solution.‡ Fig. 2 displays typical Faradaic impedance spectra (presented as Nyquist plot) of the aptamer-confined surface before (a) and after (b–e) additions of different concentrations of the lysozyme target (5–25 μg mL^{-1}; 3.5–17.5 pmol). It can be clearly observed that the electron-transfer resistance (semicircle diameter) decreases from 3.33 to 2.34 kΩ as the protein concentration is elevated. Such drop in the R_{et} is consistent with the gradually increasing positive surface charge upon increasing the protein concentration, *i.e.*, growing electrostatic attraction of

Departments of Chemical and Material Engineering and Chemistry and Biochemistry, The Biodesign Institute, Arizona State University, Tempe, AZ 85287-5801, USA. E-mail: joseph.wang@asu.edu; Tel: 1-480-727-0399

† Electronic supplementary information (ESI) available: Related instrumentation, reagents, immobilization schemes and procedures. See http://dx.doi.org/10.1039/b506571b

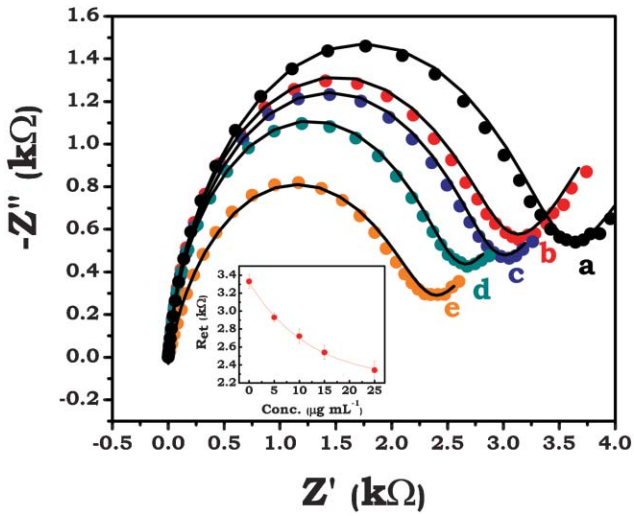

Fig. 2 Impedance sensing of protein–aptamer interactions. Typical FIS response recorded at the anti-lysozyme aptamer-modified ITO electrode in the presence of increasing concentrations of lysozyme: 0 (a), 5 (b), 10 (c), 15 (d), and 25 (e) μg mL^{-1}, along with the corresponding calibration plot (inset). The impedance spectra were recorded in a 2 mM $[Fe(CN)_6]^{3-/4-}$ (1 : 1)–0.1 M KCl–10 mM phosphate buffer (pH 7.0) solution, using a frequency range of 100 kHz–10 mHz, a bias potential of +0.225 V and an AC amplitude of 5 mV, following a 1 hour incubation with the protein solution and a 20 min wash step. The solid lines reflect the theoretical fitting in accordance with the equivalent circuit of Fig. 1C.

the electroactive marker. The resulting dependence of the sensor response on the lysozyme concentration displays a curvature, with a rapid decrease in R_{et} at first between 0 and 10 μg mL^{-1} lysozyme and a slower decay at higher concentrations. We were able to reproducibly detect the binding of 140 fmol lysozyme in the 10 μL sample (*i.e.* obtained a well defined response for a 0.2 μg mL^{-1} protein solution).

The impedance data were fitted to a Randles equivalent circuit (Fig. 1, C), that includes the solution resistance (R_s), the resistance for electron transfer (R_{et}), the constant phase element (Q_{dl}) and the Warburg impedance element (W). As indicated from Table 1, the data validation, carried out by the Kramers–Kronig test, proves that experimental results fit reasonably and are in a good agreement with the proposed circuit model ($\chi^2 < 10^{-5}$, Fig. 1C). While the W element gives information about the diffusion of $[Fe(CN)_6]^{3-/4-}$ through the surface layer, the R_s values depend only on the solution and the distance between the working and reference electrodes. Q_{dl} models the capacitive behavior of the double layer replacing the infrequently ideal capacitance and diffusion behavior; however, the deviations from an ideal capacitance ($n = 1$) are reasonably small. On the other hand, the collected data after the aptamer–protein interaction show that the R_{et} values are significantly smaller than that before the

Table 1 Values of the equivalent circuit parameters of the fitting curves for 0 and 10 μg mL^{-1} lysozyme

Lysozyme/μg mL^{-1}	R_s/kΩ	R_{et}/kΩ	Q_{dl}/Ω^{-1} s^n $Y_0/10^{-6}$	n	$W/10^{-3}$
0	1.08	3.33	0.577	0.9522	0.379
10	1.05	2.75	0.598	0.9589	0.395

interaction (Table 1), *e.g.*, decreasing from 3.33 kΩ to 2.34 kΩ, upon increasing the target concentration from 0 to 25 μg mL^{-1}, reflecting the less hindered charge transfer/marker diffusion. Very small changes are observed for the Q_{dl} and W values.

The high specificity of the method is illustrated in Fig. 3. For this purpose, the aptamer-functionalized ITO electrode was exposed to the target lysozyme solution (e) as well as to a large (4-fold) excess of different proteins [albumin (b), cytochrome C (c) and thrombin (d)]. While the presence of excess of these proteins has a negligible (~1%) effect upon the electron transfer resistance of $[Fe(CN)_6]^{3-/4-}$, binding of the lysozyme target results in a defined response, with a substantial (12%) drop of R_{et} from 3.33 to 2.92 kΩ. See inset for summary of this specificity data. Such discrimination against excess of unwanted proteins indicates minimal non-specific binding and adsorption effects, and reflects the protective action of the polymeric surface layer and the effective washing step. The high sensitivity and selectivity are coupled to good reproducibility, *e.g.* a relative standard deviation of 4% for six repetitive measurements of a 5 μg mL^{-1} lysozyme solution.

In conclusion, we demonstrated a label-free FIS biosensing of proteins based on the opposite charge of the aptamer probe and the target protein. The selective protein binding thus reverses the surface charge, hence leading to switching from repulsion to attraction of the redox marker, and to a sensitive FIS detection. An opposite effect (*i.e.*, a larger electron-transfer resistance) is expected in connection to a cationic (*e.g.*, ruthenium hexamine) redox marker. The concept can be readily extended to the aptamer-based detection of a wide range of proteins, based on tailoring the pH of the system for the individual target protein (*i.e.*, to below its pI). The successful realization of the new protocol requires proper attention to non-specific adsorption issues common to bioaffinity assays of complex matrices. To our knowledge, this is the first example of using impedance spectroscopy for monitoring aptamer interactions. It is expected that the new protocol will promote the exploitation of aptamer biosensors

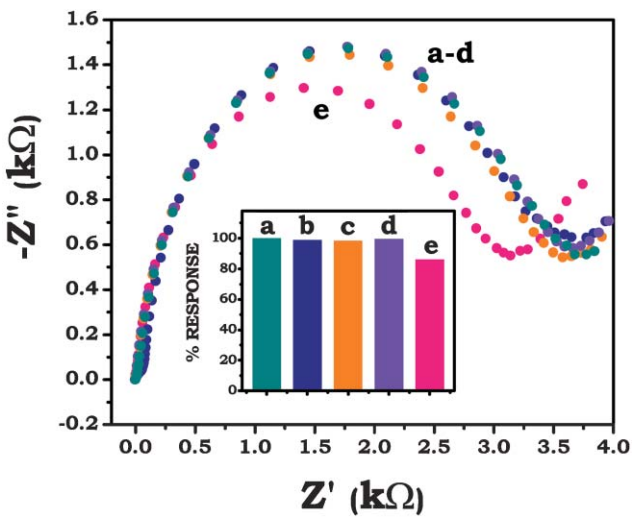

Fig. 3 Specificity of the FIS aptamer biosensor: Nyquist plots obtained for the blank solution (a), in the presence of 20 μg mL^{-1} (b) bovine serum serum, (c) cytochrome C, or (d) thrombin, and (e) 5 μg mL^{-1} lysozyme. Also shown (inset) is the corresponding bar-plot. Conditions, as in Fig. 2.

for protein assays, will speed up the diagnosis of diseases or sensing of toxins, and be adapted to rapid, high-throughput parallel protein detection. Because the transduction method is electronic, the system could be readily miniaturized. Given that aptamer-based electrochemical biosensors represent an unexplored field, we expect many exciting opportunities for aptamer-based bioelectronic devices. Particularly attractive for such future applications are label-free electronic detection schemes based on protein-induced conformational changes in the aptamer ligand.

This work was supported by the National Science Foundation (Grant Number CHE 0209707) and the NIH (Award Number R01A 1056047-01). MCR acknowledges a fellowship from Fundacion Antorchas (Argentina).

Notes and references

‡ A streptavidin-coated electrode was used for immobilizing the biotinylated anti-lysozyme aptamer.

1 T. Hermann and D. J. Patel, *Science*, 2000, **287**, 820.
2 R. Mukhopadhyay, *Anal. Chem.*, 2005, **77**, 115A.
3 L. B. McGown, M. J. Joseph, J. B. Pitner, G. P. Vonk and C. P. Linn, *Anal. Chem.*, 1995, **67**, 663A.
4 E. Baldrich, A. Restrepo and C. K. O'Sullivan, *Anal. Chem.*, 2004, **76**, 7053.
5 E. J. Merino and K. M. Weeks, *J. Am. Chem. Soc.*, 2003, **125**, 12370.
6 T. G. McCauley, N. Hamaguchi and M. Stanton, *Anal. Biochem.*, 2003, **319**, 244.
7 J. Liu and Y. Lu, *Anal. Chem.*, 2004, **76**, 1627.
8 V. Pavlov, Y. Xiao, B. Shlyabovsky and I. Willner, *J. Am. Chem. Soc.*, 2004, **126**, 11768.
9 R. Nutio and Y. Li, *J. Am. Chem. Soc.*, 2003, **125**, 4771.
10 M. N. Stojanovic and D. M. Kolpashchikov, *J. Am. Chem. Soc.*, 2004, **126**, 9266.
11 M. Dijksma, B. Kamp, J. C. Hoogvliet and W. P. van Bennekom, *Anal. Chem.*, 2001, **73**, 901.
12 C. Ruan, L. Yang and Y. Li, *Anal. Chem.*, 2002, **75**, 4814.
13 A. Bardea, E. Katz and I. Willner, *Electroanalysis*, 2000, **12**, 1097.
14 P. G. Righetti, G. Tudor and K. Ek, *J. Chromatogr.*, 1981, **220**, 115.